

Jorge López-Pérez and Jorge Íñiguez

Institut de Ciència de Materials de Barcelona (CSIC), Campus UAB, 08193 Bellaterra, Spain

We present a first-principles investigation of ferroelectricity in layered perovskite oxide $\text{La}_2\text{Ti}_2\text{O}_7$ (LTO), one of the compounds with highest Curie temperature known (1770 K). Our calculations reveal that LTO's ferroelectric transition results from the condensation of two soft modes that have the same symmetry and are strongly coupled anharmonically. Further, the leading instability mode essentially consists of rotations of the oxygen octahedra that are the basic building block of the perovskite structure; remarkably, because of the particular topology of the lattice, such O_6 rotations give rise to a spontaneous polarization in LTO. The effects discussed thus constitute an example of how nano-structuring – provided here by the natural layering of LTO – makes it possible to obtain a significant polar character in structural distortions that are typically non-polar. We discuss the implications of our findings as regards the design of novel multifunctional materials. Indeed, the observed proper ferroelectricity driven by O_6 rotations provides the ideal conditions to obtain strong magnetoelectric effects.

PACS numbers: 77.84.-s, 61.50.Ah, 75.85.+t, 71.15.Mb

I. INTRODUCTION

Because of their physical appeal and technological importance, ferroelectrics and related materials have been the object of continued attention for decades.¹⁻³ Bulk oxides with the ideal perovskite structure – ranging from classic ferroelectric BaTiO_3 to strong dielectric $\text{Ba}_{1-x}\text{Sr}_x\text{TiO}_3$, or from piezoelectric $\text{PbZr}_{1-x}\text{Ti}_x\text{O}_3$ to relaxor $(\text{PbMg}_{1/3}\text{Nb}_{2/3}\text{O}_3)_{1-x}(\text{PbTiO}_3)_x$ – have been especially well studied. Indeed, partly thanks to a number of key contributions from first-principles theory,⁴ we now understand the fundamental atomistic origin of the ferroelectric (FE) and response properties of the most important members of this family. During the past decade, the focus has increasingly shifted towards nano-structured materials, especially in the form of thin films. Work on films has led to a better understanding of how elastic (i.e., the epitaxial strain exerted by a substrate) and electric (e.g., the imperfect screening of the depolarizing field associated to particular metallic electrodes) boundary conditions affect the FE state.⁵ Further, it has been shown that exotic FE properties can be obtained in artificially created super-lattices, as e.g. in the recently discussed $\text{PbTiO}_3/\text{SrTiO}_3$ heterostructures.⁶

The emergence of magnetoelectric multiferroics⁷ (i.e., materials with coupled magnetic and FE orders) has contributed to refuel interest in ferroelectrics, especially in what regards *unconventional* mechanisms for ferroelectricity. If we restrict ourselves to oxides with the ideal ABO_3 perovskite structure, ferroelectricity (usually driven by a B -site transition metal with an nd^0 electronic configuration) and magnetism (which requires localized d or f electrons) seem to be mutually exclusive, the known exceptions being very scarce.^{8,9} So far, the most notable ways around this problem consist in (i) having ferroelectricity driven by the A -site cation, as in room temperature multiferroic BiFeO_3 ,¹⁰ and (ii) moving away from the ideal perovskite structure and resorting to other mechanisms for ferroelectricity, as e.g. in the improper

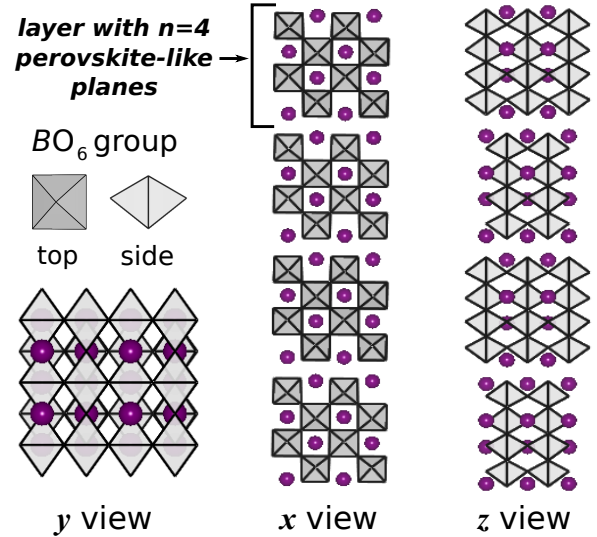


FIG. 1: (Color on-line.) Different views of the layered perovskite structure of the $A_n B_n O_{3n+2}$ compounds for $n = 4$, where n is the number of perovskite-like planes within a layer. Only the A atoms (as balls) and BO_6 octahedra are shown. The defined Cartesian axes x , y , and z (which follow the convention adopted in Ref. 32) are used throughout the paper.

ferroelectrics YMnO_3 ^{11,12} and $\text{Ca}_3\text{Mn}_2\text{O}_7$.¹³

This is the context of our work on the layered perovskite oxide $\text{La}_2\text{Ti}_2\text{O}_7$ (LTO), whose structure is sketched in Fig. 1. LTO is one of the highest-temperature ferroelectrics known, with a Curie point (T_C) of approximately 1770 K,¹⁴ and is lately being considered for applications as a high- T piezoelectric.^{15,16} The FE transition temperature of LTO is enormous, especially when compared with the T_C 's of cubic perovskite titanates one might have expected to be similar to LTO: most significantly, BaTiO_3 (BTO) becomes ferroelectric at about 400 K, and the related compound SrTiO_3 remains (a quantum) paraelectric down to 0 K. In order to explain

the surprising behavior of LTO, we need to identify the atomistic origin of its FE instability. LTO might owe its very high T_C to the kind of mechanisms known to operate in the cubic titanates (in essence, long-range dipole-dipole interactions that destabilize the non-polar phase^{17,18}), which might somehow be enhanced by the peculiar topology of the LTO lattice. Alternatively, LTO might present some new form of very strong FE instability. Either way, the study of LTO will provide us with information that might be useful for the design of new ferroelectrics.

Let us also note that LTO is a member of the family of oxides with general formula $\text{La}_n\text{Ti}_n\text{O}_{3n+2}$,¹⁹ whose structure can be seen as the ideal cubic perovskite periodically truncated along the $[011]_c$ direction of the cubic lattice, n being the number of perovskite-like planes within one layer (see Fig. 1). These structures are thus related to the well-known Ruddlesden-Popper, Aurivillius, and Dion-Jacobson families of layered perovskites,²⁰ for which the truncation direction is $[001]_c$ and which include very famous members such as $(\text{La,Ba})_2\text{CuO}_4$, the parent compound of high- T_C superconductors. The basic features of the electronic structure of the $\text{La}_n\text{Ti}_n\text{O}_{3n+2}$ compounds are controlled by n : The La and O atoms can be assumed to be in their most common ionization states – i.e., La^{3+} and O^{2-} , which implies that the Ti cations will present a positive charge of $3 + 4/n$. Accordingly, the number of $3d$ electrons in the Ti atoms will be $1 - 4/n$, which allows us to move quasi-continuously from the $\text{Ti-}3d^0$ configuration of the $n=4$ compound (that is our $\text{La}_2\text{Ti}_2\text{O}_7$, the family member with smallest n reported in the literature) to the $\text{Ti-}3d^1$ configuration of the $n=\infty$ compound (which has the prototype perovskite structure). The variety of electronic phenomena observed for intermediate values of n – including phases of semi-conducting, normal metallic, and low-dimensional metallic character¹⁹ – constitutes an additional motivation to study in detail the structural behavior of the relatively simple end member $\text{La}_2\text{Ti}_2\text{O}_7$.

The paper is organized as follows. In Section II we describe the theoretical approach and first-principles methods used in this work. We present and discuss our results in Section III, which is split in the following way. In Section III.A we describe our results for the structure of the high-temperature paraelectric (PE) and FE phases of LTO. In Section III.B we show that the PE phase presents a strong FE instability whose *topological* nature is discussed in detail. In Section III.C we describe the phase transition between the PE and FE phases, and discuss the energetics of the transformation. In Section III.D we present our results for the spontaneous polarization, dielectric, and piezoelectric properties. Having established LTO’s peculiarity, which is made manifest by means of a detailed comparison with prototype compound BTO, in Section III.E we show that LTO also presents some features that are clearly reminiscent of the usual FE oxides with the ideal perovskite structure. In Section III.F we outline the exciting implications

that our results have for the design of novel magneto-electric materials. Finally, in Section IV we summarize and present our conclusions. Whenever it is possible, we compare our first-principles results with the (scarce) experimental information available for LTO.

II. METHODOLOGY

A. Theoretical approach to $\text{La}_2\text{Ti}_2\text{O}_7$

We adopted the usual first-principles approach to the investigation of structural phase transitions of the displacive type, which is routinely applied with great success to FE perovskite oxides.²¹ Here we describe a simplified version of such an approach that is sufficient for our study of LTO (i.e., we will assume one-dimensional instability modes, will not discuss how to deal with cell strains, etc.). In essence, one needs to identify a reference equilibrium phase of high symmetry (HS) – which corresponds to the high-temperature PE phase of the compound – and study its stability against all possible structural distortions. More precisely, one writes the energy of the crystal as the following Taylor series:

$$E = E^0 + \frac{1}{2} \sum_{m,n} K_{mn} u_m u_n + \mathcal{O}(u^3), \quad (1)$$

where E^0 is the energy of the HS phase. The u_m variables represent the structural distortions of the reference configuration; for the study of a FE transition, one can typically restrict oneself to the distortions compatible with the reference unit cell, i.e., those associated to the Γ -point of the Brillouin zone of the PE phase. The so-called *force-constant matrix* \mathbf{K} is the central quantity one needs to compute, as its negative eigenvalues (if any) correspond to unstable structural distortions – i.e., *soft modes* – that may result in a phase transition. Let us use the term *mode stiffness* to refer to the eigenvalues of \mathbf{K} , which we denote by κ_s with s running from 1 to the dimension of the force-constant matrix. Note that the magnitude of a negative κ_s determines the *strength* of the structural instability, and thus the likelihood of observing it experimentally. (In general, one may find several, possibly competing, instabilities of a HS phase; it is by no means guaranteed that all of them will lead to experimentally observable phase transitions.) Once a soft mode is identified, one can readily study the corresponding low-symmetry (LS) phase – by distorting the crystal according to the soft mode eigenvector and relaxing the resulting structure – and the energetics of the instability – by computing the usual double-well potential connecting the HS and LS phases.

In order to apply this program to LTO, we had to tackle one fundamental difficulty: We could not find any experimental information on the structure of the high-temperature PE phase of this compound.²² Note that this is never a problem when one works with the usual FE

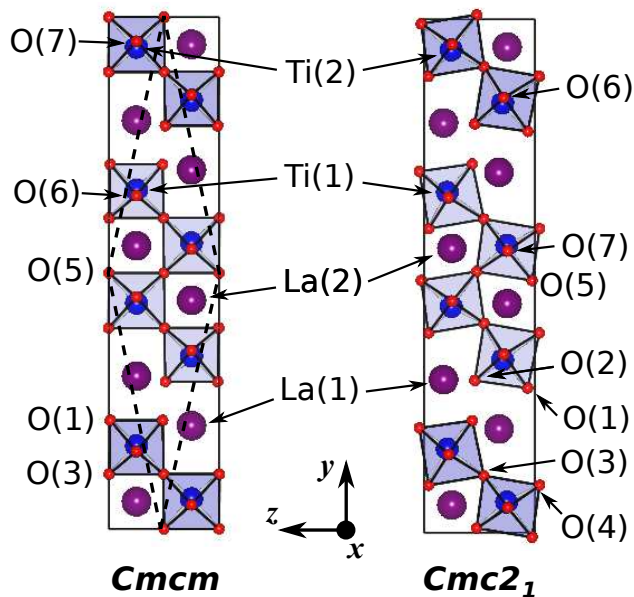


FIG. 2: (Color on-line.) Structures of the $Cmc2_1$ (FE) and $Cmcm$ (PE) phases of $\text{La}_2\text{Ti}_2\text{O}_7$ studied in this work. The small (red), medium (blue), and big (violet) balls represent O, Ti, and La atoms, respectively. The shaded polyhedra are top-viewed O_6 groups. The two phases have the same 44-atom conventional cell depicted in the figure; the 22-atom unit cell, which is also common to both, is indicated with dashed lines in the $Cmcm$ case. The defined Cartesian axes x , y , and z (which follow the convention adopted in Ref. 32) are used throughout the paper. The symmetry-independent atoms are labeled as in Table I; note that oxygens O(1) and O(3) of the $Cmcm$ structure split, respectively, into O(1)/O(2) and O(3)/O(4) in the $Cmc2_1$ structure.

perovskites, where the ideal cubic perovskite structure is the reference phase of choice. Such a choice is obviously correct in cases like those of BTO or PbTiO_3 , where the cubic PE phase is experimentally accessible for $T > T_C$; more remarkably, this choice is also the most physically sound one for materials (e.g., BiFeO_3) whose cubic PE phase is not easy to access experimentally, as the samples tend to melt before reaching the corresponding transition temperature. In the general case, the problem of choosing an appropriate HS reference phase for the theoretical study of displacive phase transitions has long been solved. The basic idea is to look for *pseudo-symmetries* (i.e., *slightly* broken symmetries) of the known LS structure; we can thus identify possible HS phases that would transform into the known LS structure upon a relatively small distortion. This is a very powerful strategy that can lead to the discovery of complex phase transition sequences (e.g., when more than one possible HS phases are found) and, in particular, has been used to identify previously unnoticed FE transitions.^{23,24}

Using widely available crystallographic tools,²⁵ we applied the pseudo-symmetry analysis to LTO and obtained a very clear prediction: We found that the FE phase of this compound, which presents space group $Cmc2_1$ and

a 22-atom primitive unit cell, is most likely associated to a PE phase with the same primitive cell and space group $Cmcm$ (see sketch in Fig. 2). We thus performed our first-principles study using this $Cmcm$ phase as our HS reference structure.

A few additional points are in order: (1) The pseudo-symmetry analysis resulted in relatively large atomic displacements connecting the HS and LS phases, with maximum values of about 0.4 Å corresponding to the La atoms. Note that the magnitude of such distortions is expected to reflect the associated HS-LS transition temperature,²⁶ which is indeed very high in this case. (2) Experimental studies of the compounds $\text{Sr}_2\text{Nb}_2\text{O}_7$ and $\text{Ca}_2\text{Nb}_2\text{O}_7$,^{27,28} which share with LTO the same layered structure and a similar (nd^0) electronic configuration of the transition metal atoms, show that they present a high-temperature phase with $Cmcm$ space group. (3) The choice of $Cmcm$ as our PE space group results in specific predictions for the symmetry of the soft modes that would be associated with a FE transition to the $Cmc2_1$ phase. Indeed, the leading instability should transform with the B_{1u} irreducible representation of mmm , the point group of the $Cmcm$ phase. As we will see, our first-principles results confirmed these expectations, thus supporting our choice of space group for the PE phase.

B. Details of the calculations

We used the local density approximation (LDA) to density functional theory (DFT) as implemented in the first-principles package VASP.²⁹ To represent the ionic cores we used the projector-augmented wave scheme,³⁰ solving explicitly for the following electrons: La's $5p$, $5d$, and $6s$; Ti's $3p$, $3d$, and $4s$; and O's $2s$ and $2p$. The electronic wave functions were represented in a plane-wave basis truncated at 400 eV. We always worked with the 44-atom cell of LTO sketched in Fig. 2 (which is the conventional cell for both $Cmcm$ and $Cmc2_1$ phases), and used a $6 \times 1 \times 5$ k -point grid for Brillouin zone integrations. We checked these calculation conditions were well-converged by monitoring the computed equilibrium structure, bulk modulus, and phonon frequencies of the $Cmcm$ phase. For the calculation of the force-constant matrix \mathbf{K} and the dielectric and piezoelectric responses, we employed a simple finite-displacement scheme and the corresponding linear-response tensor formulas, which can be found e.g. in Ref. 31. We only computed the lattice-mediated part of the static dielectric response, which has been repeatedly shown to dominate the effect in ferroelectric oxides.

Our BTO simulations were analogous to the above described ones. We solved explicitly for Ba's $5s$, $5p$, and $6s$ electrons (treating Ti and O as above), and used a 400 eV cut-off for the plane-wave basis. We worked with the 5-atom unit cell of BTO, and used a $6 \times 6 \times 6$ k -point grid for Brillouin zone integrations.

III. RESULTS AND DISCUSSION

A. Structure of the $Cmcm$ and $Cmc2_1$ phases

Table I shows our results for the equilibrium structure of the $Cmcm$ (PE) and $Cmc2_1$ (FE) phases of LTO considered in this study. For $Cmc2_1$ we also report the experimental structure measured at 1173 K by Ishizawa *et al.*³² using X-ray diffraction.

While the overall agreement between the experimental and theoretical FE structures is acceptable, the deviations affecting some atomic positions and lattice constants are larger than what is usual for this type of calculations. For example, the predicted position of the La(1) atom differs notably from the experimentally determined one; more significantly, the computed a and c lattice constants deviate from the experimental values by almost a 3%. We attribute these discrepancies to the fact that we are comparing our first-principles results, which correspond to the limit of 0 K, with structural data taken at very high temperatures. Given that thermal expansion and other temperature-driven effects are not included in our simulations, our results seem compatible with the experimental information.

B. Ferroelectric instabilities of the $Cmcm$ phase

As described in Section II.A, we studied the structural stability of the $Cmcm$ phase against Γ -point distortions (compatible with the PE unit cell) by computing the corresponding force-constant matrix \mathbf{K} . From the diagonalization of \mathbf{K} we obtained two negative eigenvalues that correspond to two structural instabilities. The computed mode stiffnesses are -0.81 eV/Å² and -0.01 eV/Å², respectively. Hence, according to our calculations, LTO's $Cmcm$ phase presents a structural instability comparable in strength with the FE soft mode of BTO's PE phase (for which we obtained -2.74 eV/Å²), as well as a marginally unstable mode with nearly zero stiffness.

Both instabilities transform with the B_{1u} irreducible representation of the mmm point group of the PE phase; more precisely, they are infra-red active (polar) modes that involve the development of a polarization along the z direction defined in Fig. 2. Such B_{1u} modes break the C_{2y} , C_{2x} , I , and σ_z point symmetries of the PE phase (where I is the spatial inversion, $C_{2\alpha}$ stands for a two-fold rotation around axis α , and σ_α is a mirror plane perpendicular to direction α), leading to the $Cmc2_1$ space group. Hence, the obtained B_{1u} soft modes are exactly the kind of instabilities that can drive a ferroelectric phase transition between the $Cmcm$ and $Cmc2_1$ phases. Our first-principles results thus support the correctness of our working hypothesis, i.e., that the studied $Cmcm$ structure is indeed the high-symmetry PE phase of LTO.

We can gain insight into the origin of ferroelectricity in LTO by inspecting the eigenvector of the strongest instability mode, denoted by ξ_1 in the following. In essence,

TABLE I: Computed equilibrium structures of the $Cmcm$ and $Cmc2_1$ phases of $\text{La}_2\text{Ti}_2\text{O}_7$ discussed in the text. We show in parenthesis the experimental values reported in Ref. 32 for the $Cmc2_1$ phase.

$Cmcm$				
		$a = 3.891 \text{ \AA}$	$b = 25.720 \text{ \AA}$	$c = 5.465 \text{ \AA}$
		$\alpha = \beta = \gamma = 90^\circ$		
Atom	Wyc.	x	y	z
La(1)	4c	0	0.2924	1/4
La(2)	4c	0	0.4453	3/4
Ti(1)	4c	1/2	0.3389	3/4
Ti(2)	4c	1/2	0.4437	1/4
O(1)	8f	1/2	0.2881	0.9931
O(3)	8f	1/2	0.3982	0.9869
O(5)	4a	1/2	1/2	1/2
O(6)	4c	0	0.3458	3/4
O(7)	4c	0	0.4525	1/4
$Cmc2_1$				
		$a = 3.845 \text{ \AA}$	$b = 25.626 \text{ \AA}$	$c = 5.464 \text{ \AA}$
		$(a = 3.954 \text{ \AA})$	$(b = 25.952 \text{ \AA})$	$(c = 5.607 \text{ \AA})$
		$\alpha = \beta = \gamma = 90^\circ$		
Atom	Wyc.	x	y	z
La(1)	4a	0	0.2978	0.1675
			(0.2981)	(0.1757)
La(2)	4a	0	0.4464	0.7515
			(0.4461)	(0.7500)
Ti(1)	4a	1/2	0.3369	0.7069
			(0.3370)	(0.7095)
Ti(2)	4a	1/2	0.4407	0.2422
			(0.4404)	(0.2452)
O(1)	4a	1/2	0.2803	0.9245
			(0.2818)	(0.9350)
O(2)	4a	1/2	0.2960	0.4399
			(0.2964)	(0.4580)
O(3)	4a	1/2	0.3843	0.0415
			(0.3891)	(0.0390)
O(4)	4a	1/2	0.4072	0.5549
			(0.4077)	(0.5420)
O(5)	4a	1/2	0.4905	0.9724
			(0.4912)	(0.9750)
O(6)	4a	0	0.3460	0.7426
			(0.3472)	(0.7200)
O(7)	4a	0	0.4507	0.2604
			(0.4511)	(0.2550)

ξ_1 involves a rotation of the O₆ oxygen octahedra around the x axis, as sketched in Fig. 3(a). Hence, the displacements of the equatorial oxygens amount to most of the eigenvector (11% of the norm of ξ_1 is associated to O(1) displacements, 51% to O(3), and 28% to O(5), using the

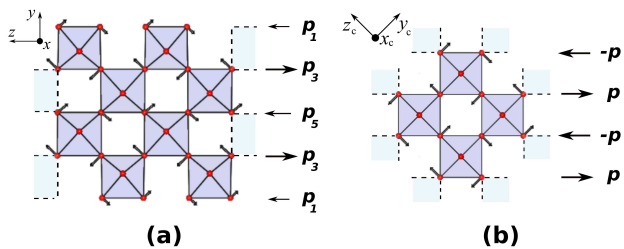


FIG. 3: (Color on-line.) Panel (a): sketch of the largest atomic displacements associated to the strongest instability mode (ξ_1) obtained for the $Cmcm$ phase of $La_2Ti_2O_7$. We show the displacements corresponding to one layer composed of $n = 4$ perovskite-like planes. The arrows on the side represent the electric dipoles associated to the displacement of oxygens in different y -planes (see text). The dipoles are labeled as the oxygen atoms in Fig. 2. Panel (b): sketch of a typical anti-ferrodistortive mode occurring in an ideal (non-layered) perovskite structure.

labels defined in Fig. 2 for the oxygen atoms); there are also significant La displacements (9% of the norm), while the Ti atoms and apical oxygens O(6) and O(7) have a negligible participation in ξ_1 . The character of the second soft mode (ξ_2) is more complex: It is dominated by the displacements of oxygens O(1) and O(5) (with 21% and 35% of the norm, respectively) and involves a significant deformation of the O_6 octahedra; it also presents a large participation of the La atoms (about 24% of the norm).

These FE instabilities are very different from the ones that are usual among ABO_3 oxides with the ideal perovskite structure. The inset of Fig. 4(b) shows the representative case of BTO: the Ti cation moves away from the center of the O_6 octahedron, which is only slightly distorted, giving raise to a large electric dipole. Further, the FE instability in BTO and related materials is known to originate from the strong interactions between such local dipoles.¹⁸ In contrast, the dominant FE instability found in LTO consists of O_6 octahedra rotations, the off-centering of the Ti atoms being negligible. As quantified in Section III.D, such a pattern of atomic displacements does not lead to a large local dipole, which suggests that the mechanisms responsible for the ferroelectricity in LTO have to be of a different nature.

Interestingly, structural instabilities involving O_6 octahedra rotations are very common among ABO_3 perovskites, and are usually termed anti-ferrodistortive (AFD). Indeed, AFD modes as the one sketched in Fig. 3(b) are the driving force for most of the structural phase transitions occurring in these compounds, the examples including crystals as well-known as $SrTiO_3$, $LnMnO_3$ and $LnNiO_3$ (where Ln is a lanthanide), multiferroics $BiMO_3$ (where M is a $3d$ transition metal), etc. Accordingly, there is extensive literature devoted to the study and classification AFD modes in ABO_3 perovskites,^{33,34} and it is known that size (e.g., the incompatibility of the ionic radii of the A and B cations

to form a cubic perovskite lattice) and chemical (as in the Bi-based compounds that display the so-called *stereochemical activity*) effects are usually responsible for the occurrence of AFD distortions.³⁵ Hence, it is not a surprise to find that layered perovskite structures may present AFD-like instabilities that allow for a better fulfillment of steric and/or chemical constraints at a local level. It is not our goal here to discuss the occurrence and origin of such soft modes in LTO-like layered perovskites; such a study should probably involve consideration of a number of representative crystals (e.g., a few members of the $A_nB_nO_{3n+2}$ family) and falls beyond the scope of this work. Suffice it to say that the leading FE instability that we found in LTO is essentially analogous to the AFD distortions that are ubiquitous among perovskite oxides.

However, we must note a critical difference between LTO's AFD-like mode depicted in Fig. 3(a) and the AFD modes occurring in ideal perovskite structures [Fig. 3(b)]: the former causes a spontaneous polarization, while the latter do not. To better explain this, in Fig. 3(a) we indicate with arrows the electric dipoles that appear as a consequence of the displacement of the oxygen atoms following the ξ_1 eigenvector. The oxygens in each y -oriented plane give raise to a dipole along the z direction. Using the definitions in Fig. 3(a), the total dipole associated to one layer would be $\mathbf{p}^{\text{layer}} = \mathbf{p}_5 + 2\mathbf{p}_3 + 2\mathbf{p}_1$. Since there is no symmetry relationship between the displacements of the O(1), O(3), and O(5) oxygens in the ξ_1 eigenvector, it follows immediately that $\mathbf{p}^{\text{layer}}$ will be different from zero. Moreover, even if oxygens of different types were to displace by the same amount, so that $\mathbf{p}_5 = -\mathbf{p}_3 = \mathbf{p}_1 = \mathbf{p}$, we would still have $\mathbf{p}^{\text{layer}} = \mathbf{p} \neq 0$, as the number of oxygen planes in each layer is odd. Finally, note that LTO's unstable mode ξ_1 involves an identical distortion of all layers in the structure, and thus gives raise to a net macroscopic polarization.

On the other hand, AFD distortions of the ideal (non-layered) perovskite structure do not result in a macroscopic polarization. In Fig. 3(b) we show a pattern of O_6 rotations around the indicated x_c axis; the situation is very similar to the one depicted in Fig. 3(a), except that in this case the network of O_6 octahedra is not truncated. Again, we indicate with arrows the electric dipoles that appear as a consequence of the oxygen displacements: oxygens within a $[011]_c$ -oriented plane give raise to a dipole \mathbf{p} along $[01\bar{1}]_c$. It is apparent that the addition of all such dipoles gives no net polarization in this case, a result that can be viewed as a consequence of the three-dimensional nature of the O_6 network.

In conclusion, we have found that the strongest structural instability in LTO's high-symmetry phase is a very common and simple one: it involves concerted rotations of the O_6 octahedra, much alike the AFD modes responsible for the structural phase transitions in most ABO_3 crystals with the ideal perovskite structure. AFD distortions in the usual perovskites are well-known to be non-polar, a feature that can be viewed as a consequence

TABLE II: Energy difference between the FE and PE phases of $\text{La}_2\text{Ti}_2\text{O}_7$ and BaTiO_3 . The FE phases are considered under several elastic constraints (see text), which we denote “fully-relaxed” (no constraint), “PE volume”, and “PE cell”. For both LTO and BTO, the energies are normalized to the volume of the PE phase so that a comparison between compounds can be made. Results given in $\text{meV}/\text{\AA}^3$.

	$\text{La}_2\text{Ti}_2\text{O}_7$	BaTiO_3
fully-relaxed	-1.097	-0.110
PE volume	-1.042	-0.099
PE cell	-0.938	-0.051

of the symmetry and three-dimensional character of the lattice. In contrast, because the structure of LTO is split in layers comprising an even number of perovskite planes, the O_6 -rotation mode gives rise to a net polarization in this case. Hence, since the occurrence of a spontaneous polarization in LTO relies on the layered topology of the lattice, it seems appropriate to describe this compound as a *topological ferroelectric*. Let us stress that LTO’s peculiar lattice topology does not seem essential for the structural instability to exist, but it is critical for it to have a polar character.

C. Nature of the $Cmcm$ -to- $Cmc2_1$ transition

In addition to the already discussed topological nature of the leading FE instability, the transformation between LTO’s $Cmcm$ and $Cmc2_1$ phases presents a number of interesting aspects that we discuss in the following. Most importantly, our results show that the transition is driven by the combined action of the two soft modes discussed in the previous Section, and suggest that such a cooperation is critical for it to occur at a very high temperature.

To study a structural phase transition quantitatively, one can start by comparing the energies of the phases involved. Table II shows our results for LTO, along with the analogous data for the $Pm\bar{3}m$ (PE) and $P4mm$ (FE) phases of BTO. Note that the energy change *per* unit volume involved in LTO’s transition is about one order of magnitude greater than the corresponding one for BTO. Such an enormous difference is compatible with the experimentally measured Curie temperatures, which are 1770 K and 400 K for LTO and BTO, respectively. Hence, our first-principles results for the energetics of LTO’s FE transition seem consistent with experiments.

Table II also contains information about the elastic deformation that accompanies the FE transitions. The properties of FE oxides with the ideal perovskite structure are known to be strongly sensitive to cell strains. This is clearly reflected in the results for BTO: If the compound is forced to keep the cubic cell of the PE structure, the energy gain involved in the FE transition is reduced by half (i.e., it drops from $-0.110 \text{ meV}/\text{\AA}^3$ to $-0.051 \text{ meV}/\text{\AA}^3$). On the other hand, if we only im-

pose the PE volume (so that the FE cell is allowed to deform and acquire a $c/a \neq 1$ ratio), the energetics of the transformation is not strongly affected. In contrast, the analogous elastic constraints have a relatively small effect in the case of LTO (i.e., the energy gain drops from $-1.097 \text{ meV}/\text{\AA}^3$ to $-0.938 \text{ meV}/\text{\AA}^3$ when we impose the PE cell). Such a weak coupling between strain and the FE distortion is probably reflecting the AFD-like character of the instability;³⁶ this result also suggests that LTO will display relatively small piezoelectric effects as compared with regular FE perovskites.

Let us now consider the atomic displacements that characterize the $Cmcm$ -to- $Cmc2_1$ transformation. In most materials undergoing displacive transitions, the atomic distortion connecting the HS and LS phases is essentially captured by the eigenvector of the instability mode that triggers the transformation. One can easily quantify this by constructing a *distortion vector* $\Delta\mathbf{X}$ comprising all the atomic displacements associated to the HS-to-LS transition, and expressing it in the basis formed by the eigenvectors ξ_s of the force-constant matrix of the HS phase. (For simplicity, we constructed our distortion vectors $\Delta\mathbf{X}$ using the atomic positions of a LS phase that is forced to have the same unit cell as the HS phase.) For BTO, this analysis led us to the expected result: the soft mode of the PE phase captures 98% of the atomic distortion involved in the $Pm\bar{3}m$ -to- $P4mm$ transition. However, the result for LTO was qualitatively different: the strongest instability mode (ξ_1 , with $\kappa_1 = -0.81 \text{ eV}/\text{\AA}^2$) captures 81% of the total distortion, and the second instability mode (ξ_2 , with $\kappa_2 = -0.01 \text{ eV}/\text{\AA}^2$) contributes with a 15%. (For both compounds, no other mode contributes more than a 1%.) Hence, our results suggest that the two soft modes ξ_1 and ξ_2 play an important role in LTO’s FE phase transition.

Such a large contribution of ξ_2 to the structural transformation seems incompatible with the computed mode stiffnesses; indeed, the values of κ_1 and κ_2 would suggest that ξ_2 is about 80 times weaker than ξ_1 as an instability. To resolve this apparent contradiction, we computed how LTO’s energy changes when the $Cmcm$ phase is distorted according to the individual ξ_1 and ξ_2 modes. As shown in Fig. 4(a), we found a large energy reduction associated with the ξ_1 distortion, while the ξ_2 instability is almost negligible. We also computed the energy variation as the total distortion $\Delta\mathbf{X}$ is frozen in. Remarkably, as compared with the results for ξ_1 , the $\Delta\mathbf{X}$ curve in Fig. 4(a) presents a much deeper minimum corresponding to a much larger distortion amplitude. This is a new indication that the ξ_1 soft mode cannot explain LTO’s FE transition by itself. This result contrasts with the situation for BTO [Fig. 4(b)], where the FE soft mode captures the energetics of the structural transformation almost exactly.

The results of Fig. 4(a) suggest that there is a strong and *cooperative* coupling between the two instability modes of LTO. To better describe this effect, let us write

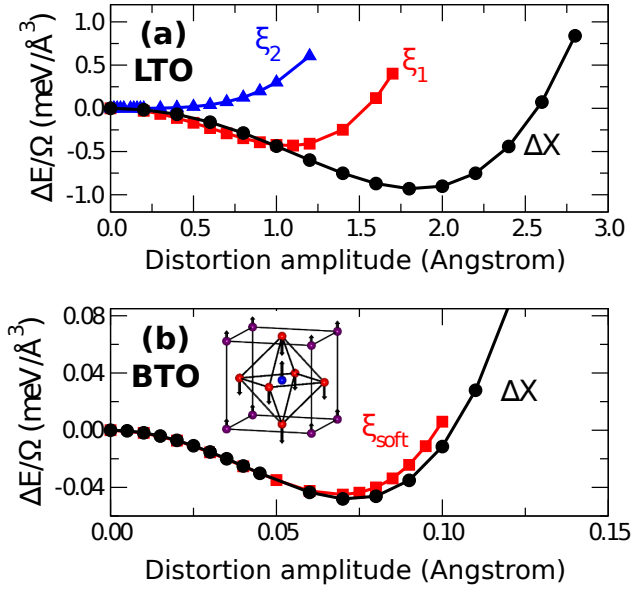


FIG. 4: (Color on-line.) Panel (a): Variation of the energy of $\text{La}_2\text{Ti}_2\text{O}_7$ as the $Cmcm$ phase is distorted according to several atomic displacement patterns, namely, those corresponding to the soft modes ξ_1 and ξ_2 , as well as the distortion $\Delta\mathbf{X}$ that connects the $Cmcm$ and $Cmc2_1$ phases. The 44-atom cell of the $Cmcm$ phase is kept fixed in all calculations. Panel (b): Same as panel (a) for the PE ($Pm\bar{3}m$) to FE ($P4mm$) transition of BaTiO_3 . The inset shows the atomic displacements associated to the single FE soft mode of BTO (Ba atoms at the corners of the cubic cell; Ti atom at the center of the O_6 octahedron). For both LTO and BTO, the energies are normalized to the volume of the PE phase so that a comparison between compounds can be made.

the energy of the crystal as the following Taylor series:

$$E = E^{Cmcm} + \frac{1}{2}\kappa_1 u_1^2 + \frac{1}{2}\kappa_2 u_2^2 + \frac{1}{4}\alpha_1 u_1^4 + \frac{1}{4}\alpha_2 u_2^4 + \gamma' u_1^3 u_2 + \gamma'' u_1^2 u_2^2 + \gamma''' u_1 u_2^3 + \mathcal{O}(u^6), \quad (2)$$

where E^{Cmcm} is the energy of the $Cmcm$ phase, and u_1 and u_2 are, respectively, the amplitudes (in Angstrom) of the ξ_1 and ξ_2 distortions. Note that this expression for the energy is greatly simplified by symmetry, and that the quadratic parameters coincide with the mode stiffnesses. We have included in Eq. (2) only the lowest-order couplings between u_1 and u_2 , which are quantified by the primed γ parameters. By fitting to the ξ_1 and ξ_2 energy curves of Fig. 4(a), we got $\kappa_1 = -0.79 \text{ eV}/\text{\AA}^2$ and $\kappa_2 = 0.00 \text{ eV}/\text{\AA}^2$, in fair agreement with the values obtained from the diagonalization of \mathbf{K} ; we also got $\alpha_1 = 0.65 \text{ eV}/\text{\AA}^4$ and $\alpha_2 = 0.66 \text{ eV}/\text{\AA}^4$. Then, to fit the $\Delta\mathbf{X}$ curve we considered distortions characterized by $u_1/u_2 = 0.81/0.15$, as it corresponds to the $Cmc2_1$ phase. Note that, in this case, the fitted quartic coefficient is a combination of the α and γ parameters of Eq. (2). Given the large u_1/u_2 ratio associated with the $\Delta\mathbf{X}$ distortion, and in view of further tests discussed in Section III.D, it seems reasonable to assume that γ' dom-

inates over γ'' and γ''' ; we thus got $\gamma' = -0.35 \text{ eV}/\text{\AA}^4$. As compared with the computed α coefficients, this clearly is a very strong anharmonic coupling that favors the combined $\xi_1 + \xi_2$ distortion.³⁷

To the best of our knowledge, such a cooperation between soft modes is rare among perovskite oxides. There are many examples of materials in which several strong instabilities exist; in most cases, the strongest one leads to a phase transition that tends to suppress, partially or totally, the other instabilities. The competition between the FE and AFD soft modes in compounds like SrTiO_3 is a representative and well studied case.³⁸ In contrast, we find that the reciprocal enhancement of the two soft FE modes is critical to explain the structural transformation in LTO. The ξ_1 mode is clearly the leading instability, and it would occur even in absence of ξ_2 . Yet, as the results in Fig. 4(a) show, the magnitude and strength of the transformation are boosted by the interaction between ξ_1 and ξ_2 . Thus, our results seem to suggest that LTO owes its very high T_C to such an interaction; indeed, in view of Fig. 4(a), it is hard to imagine LTO's T_C would remain essentially the same if the coupling between ξ_1 and ξ_2 was suppressed.

Studying from first-principles the temperature dependence of the ξ_1 and ξ_2 distortions, and the details of how these two soft modes freeze in at LTO's FE transition, is a challenging endeavor that remains for future work. Nevertheless, a few observations can be made based on the present results. In principle, one could try to approach the problem by introducing a Landau potential of the form:

$$F - F_0 = \frac{1}{2}A_1(T - T_C)Q_1^2 + \frac{1}{4}B_1Q_1^4 + \frac{1}{2}A_2Q_2^2 + \frac{1}{4}B_2Q_2^4 + C'Q_1^3Q_2 + C''Q_1^2Q_2^2 + C'''Q_1Q_2^3, \quad (3)$$

which is written in terms of two one-dimensional order parameters, Q_1 and Q_2 , that have the same symmetry. In the following heuristic argument we will consider only the $Q_1^3Q_2$ crossed term – in accordance with our above conjecture regarding the couplings in Eq. (2), and because this is the most relevant crossed term in vicinity of the phase transition³⁹ – thus assuming that $C'' = C''' = 0$.

If we were dealing with a simple transition, we would have a primary order parameter Q_1 corresponding to the unstable eigenmode of the \mathbf{K} matrix of the high-symmetry phase; the temperature dependence of the Landau potential would be restricted to the Q_1^2 term, as indicated in Eq. (3), and we would have positive A_1 and B_1 coefficients. Further, a secondary order parameter Q_2 would be stable by itself, with positive A_2 and B_2 coefficients. Hence, the corresponding Landau theory would predict a phase transition at $T = T_C$, with

$$Q_1 = \left[\frac{A_1}{B_1}(T_C - T) \right]^{1/2} \quad (4)$$

below the transition temperature. (The indicated formulas were derived assuming that we remain close to the transition temperature.) Then, Q_2 would present the following temperature dependence below T_C :

$$Q_2 = -\frac{C'}{A_2}Q_1^3 = -\frac{C'}{A_2} \left[\frac{A_1}{B_1}(T_C - T) \right]^{3/2}. \quad (5)$$

In a simple case, the coefficients in Eq. (2) may be a good approximation to the coefficients in Eq. (3) in the limit of low temperatures. Thus, by supplementing the Eq. (2) deduced from first-principles with a piece experimental information – i.e., the value of the transition temperature T_C –, we could construct the corresponding Landau potential and obtain a quantitative description of the temperature dependence of Q_1 and Q_2 .

The doubts quickly appear when one tries to apply this model to LTO. It seems natural to associate Q_1 and Q_2 with our computed FE soft modes ξ_1 and ξ_2 , respectively. However, that identification implies that the transition temperature for Q_1 is independent of Q_2 ; such an approximation would be an awkward one, given the large influence that ξ_2 has in the energetics of the $Cmcm$ -to- $Cmc2_1$ transformation. Additionally, we would be forced to speculate regarding the T -dependence of the A_2 coefficient, as our *guess* for this parameter – i.e., the κ_2 of Eq. (2) which was found to be essentially zero – does not comply with the usual requirements for the quadratic coefficient of a secondary mode. Note that, for example, if we had a small value of A_2 and thus a dominant B_2 term, the behavior with temperature of both Q_1 and Q_2 would vary: Q_1 would have the same functional T -dependence but with a different prefactor, and Q_2 would go as $(T_C - T)^{1/2}$ instead of $(T_C - T)^{3/2}$. The results of this study do not allow us to resolve such details of LTO's transition.

D. Polarization and response properties

Table III shows the computed spontaneous polarization, lattice-mediated dielectric tensor, and piezoelectric tensor for the $Cmc2_1$ phase of LTO. For comparison, we also show results from the literature corresponding to the $P2_1$ phase that is stable at room temperature.

We obtained a value of 0.29 C/m² for the spontaneous polarization, which is comparable with the result of 0.38 C/m² that we obtained for the tetragonal phase of BTO. The dielectric response is also very significant, as the obtained values are comparable with those typical of FE perovskites (e.g., we got $\epsilon_{zz} = 23$ for the z -polarized tetragonal phase of BTO). As regards piezoelectricity, the computed responses are considerable but not particularly large; for example, for the low-temperature rhombohedral phase of BTO, the piezoelectric coefficients reach values of 200 pC/N,³¹ while for LTO we got maximum values of about 20 pC/N. LTO's relatively small piezoelectric response seems compatible with the minor role

TABLE III: Non-zero components of the spontaneous polarization (P_z^S , given in C/m²), lattice-mediated dielectric tensor ($\epsilon_{\alpha\beta}$), and piezoelectric tensor ($d_{\alpha l}$, where l labels strain components in Voigt notation, given in pC/N) of the $Cmc2_1$ phase of La₂Ti₂O₇. For the dielectric tensor, the clamped-cell response is given in parenthesis.³¹ For the piezoelectric tensor, the clamped-ion response is given in parenthesis. We also show experimental¹⁴ and theoretical¹⁶ values for the $P2_1$ phase of LTO that is stable at room temperature (T_{room}). Note that the results in Refs. 14 and 16 have been adapted to our choice of Cartesian axes.

	$Cmc2_1$ phase		$P2_1$ phase	
	this work	exp. (T_{room}) ¹⁴	theory ¹⁶	
P_z^S	0.29	0.05	0.08	
ϵ_{xx}	62 (61)	52	-	
ϵ_{yy}	44 (44)	42	-	
ϵ_{zz}	65 (54)	62	-	
d_{z1}	12 (0)	3	-	
d_{z2}	4 (1)	6	-	
d_{z3}	-22 (0)	16	-	
d_{x5}	-2 (0)	-	-	
d_{y4}	1 (0)	-	-	

that the cell strains play in determining the energetics of the $Cmcm$ -to- $Cmc2_1$ phase transition, as mentioned in the discussion of Table II.

The large spontaneous polarization obtained may seem incompatible with the AFD-like character of the structural instability (ξ_1) that dominates the $Cmcm$ -to- $Cmc2_1$ transition. To clarify this point, we performed alternative calculations using linear-response expressions³¹ based on the Born effective-charge tensors Z_i^* that quantify the polarization change associated to the displacement of an individual atom i .

The polarization reported in Table III was obtained in the standard way: We used the Berry-phase theory of King-Smith and Vanderbilt⁴⁰ to compute the variation of \mathbf{P} as the $Cmc2_1$ structure is deformed into a symmetry-equivalent one with opposite polar distortion; then, \mathbf{P}^S is half of the computed polarization change. \mathbf{P}^S can also be estimated using the approximate formula

$$P_\alpha^S \approx \sum_{i\beta} Z_{i,\alpha\beta}^* \Delta X_{i\beta}, \quad (6)$$

where $\Delta \mathbf{X}$ is the vector capturing the distortion that connects the $Cmcm$ and $Cmc2_1$ phases, i labels the atoms in the unit cell, and α and β label spatial directions. Using different choices for the effective-charge tensors (i.e., those computed for the $Cmcm$ phase, as well as the corresponding results for the $Cmc2_1$ phase subject to different cell constraints) we obtained values of P_z^S in the 0.25-0.32 C/m² range, which are perfectly compatible with the result in Table III.

Then, we used the effective-charge tensors of the $Cmcm$ phase (given in Table IV) to compute the polar-

TABLE IV: Computed effective-charge tensors (given in units of elementary charge) for the $Cmcm$ (PE) and $Cmc2_1$ (FE) phases of $\text{La}_2\text{Ti}_2\text{O}_7$. To facilitate the comparison between phases, we list the tensors corresponding to all the symmetry-inequivalent atoms of the FE phase. Atoms are labeled as in Table I.

	$Cmcm$ (PE)	$Cmc2_1$ (FE)
La(1)	$\begin{pmatrix} 4.63 & 0 & 0 \\ 0 & 4.17 & 0 \\ 0 & 0 & 4.72 \end{pmatrix}$	$\begin{pmatrix} 4.64 & 0 & 0 \\ 0 & 4.09 & -0.21 \\ 0 & -0.69 & 4.71 \end{pmatrix}$
La(2)	$\begin{pmatrix} 4.37 & 0 & 0 \\ 0 & 3.76 & 0 \\ 0 & 0 & 4.28 \end{pmatrix}$	$\begin{pmatrix} 4.63 & 0 & 0 \\ 0 & 4.13 & 0.41 \\ 0 & 0.24 & 4.24 \end{pmatrix}$
Ti(1)	$\begin{pmatrix} 6.91 & 0 & 0 \\ 0 & 6.70 & 0 \\ 0 & 0 & 5.72 \end{pmatrix}$	$\begin{pmatrix} 6.16 & 0 & 0 \\ 0 & 5.60 & -0.36 \\ 0 & 0.24 & 5.31 \end{pmatrix}$
Ti(2)	$\begin{pmatrix} 6.33 & 0 & 0 \\ 0 & 5.32 & 0 \\ 0 & 0 & 7.45 \end{pmatrix}$	$\begin{pmatrix} 6.11 & 0 & 0 \\ 0 & 5.29 & 0.09 \\ 0 & -0.15 & 6.32 \end{pmatrix}$
O(1)	$\begin{pmatrix} -2.52 & 0 & 0 \\ 0 & -3.20 & 0.73 \\ 0 & 0.86 & -3.26 \end{pmatrix}$	$\begin{pmatrix} -2.52 & 0 & 0 \\ 0 & -3.14 & 0.53 \\ 0 & 0.38 & -2.92 \end{pmatrix}$
O(2)	$\begin{pmatrix} -2.52 & 0 & 0 \\ 0 & -3.20 & -0.73 \\ 0 & -0.86 & -3.26 \end{pmatrix}$	$\begin{pmatrix} -2.15 & 0 & 0 \\ 0 & -2.35 & -0.89 \\ 0 & -0.90 & -3.44 \end{pmatrix}$
O(3)	$\begin{pmatrix} -2.08 & 0 & 0 \\ 0 & -3.27 & -1.72 \\ 0 & -1.56 & -3.98 \end{pmatrix}$	$\begin{pmatrix} -1.76 & 0 & 0 \\ 0 & -3.33 & -1.36 \\ 0 & -1.38 & -2.95 \end{pmatrix}$
O(4)	$\begin{pmatrix} -2.08 & 0 & 0 \\ 0 & -3.27 & 1.72 \\ 0 & 1.56 & -3.98 \end{pmatrix}$	$\begin{pmatrix} -2.49 & 0 & 0 \\ 0 & -3.19 & 1.28 \\ 0 & 1.19 & -3.64 \end{pmatrix}$
O(5)	$\begin{pmatrix} -2.49 & 0 & 0 \\ 0 & -3.15 & 1.19 \\ 0 & 0.98 & -3.64 \end{pmatrix}$	$\begin{pmatrix} -2.63 & 0 & 0 \\ 0 & -3.11 & 1.04 \\ 0 & 1.00 & -3.36 \end{pmatrix}$
O(6)	$\begin{pmatrix} -5.50 & 0 & 0 \\ 0 & -2.15 & 0 \\ 0 & 0 & -1.66 \end{pmatrix}$	$\begin{pmatrix} -5.04 & 0 & 0 \\ 0 & -2.08 & 0.24 \\ 0 & 0.14 & -1.75 \end{pmatrix}$
O(7)	$\begin{pmatrix} -5.10 & 0 & 0 \\ 0 & -1.73 & 0 \\ 0 & 0 & -2.41 \end{pmatrix}$	$\begin{pmatrix} -4.99 & 0 & 0 \\ 0 & -1.91 & -0.03 \\ 0 & -0.02 & -2.20 \end{pmatrix}$

ization change associated with the condensation of the ξ_1 and ξ_2 soft modes that dominate the $Cmcm$ -to- $Cmc2_1$ transformation. The polar character of the modes is quantified in terms of the *mode effective charges*:

$$\bar{Z}_{s,\alpha} = \sum_{i\beta} Z_{i,\alpha\beta}^* \xi_{s,i\beta}. \quad (7)$$

We obtained $\bar{Z}_{1,z} = 1.8e$ and $\bar{Z}_{2,z} = 12.0e$, where e is the elemental charge. These results confirm that the ξ_1 is weakly polar, in accordance with its AFD-like nature. In

TABLE V: Computed effective-charge tensors (given in units of elementary charge) for the $Pm\bar{3}m$ (PE) and $P4mm$ (FE) phases of BaTiO_3 . The tensors are given in the conventional Cartesian axes for a rectangular lattice. They correspond to the following atoms (PE phase positions given in relative units): Ba located at (0,0,0), Ti at (1/2,1/2,1/2), O(1) at (1/2,1/2,0), and O(2) at (0,1/2,1/2). O(1) and O(2) are symmetry-equivalent in the PE phase, but not in the z -polarized FE phase.

	$Pm\bar{3}m$ (PE)	$P4mm$ (FE)
Ba	$\begin{pmatrix} 2.72 & 0 & 0 \\ 0 & 2.72 & 0 \\ 0 & 0 & 2.72 \end{pmatrix}$	$\begin{pmatrix} 2.71 & 0 & 0 \\ 0 & 2.71 & 0 \\ 0 & 0 & 2.81 \end{pmatrix}$
Ti	$\begin{pmatrix} 7.31 & 0 & 0 \\ 0 & 7.31 & 0 \\ 0 & 0 & 7.31 \end{pmatrix}$	$\begin{pmatrix} 7.05 & 0 & 0 \\ 0 & 7.05 & 0 \\ 0 & 0 & 5.83 \end{pmatrix}$
O(1)	$\begin{pmatrix} -2.13 & 0 & 0 \\ 0 & -2.13 & 0 \\ 0 & 0 & -5.77 \end{pmatrix}$	$\begin{pmatrix} -1.98 & 0 & 0 \\ 0 & -1.98 & 0 \\ 0 & 0 & -4.79 \end{pmatrix}$
O(2)	$\begin{pmatrix} -5.77 & 0 & 0 \\ 0 & -2.13 & 0 \\ 0 & 0 & -2.13 \end{pmatrix}$	$\begin{pmatrix} -5.62 & 0 & 0 \\ 0 & -2.14 & 0 \\ 0 & 0 & -1.96 \end{pmatrix}$

contrast, the second soft mode ξ_2 is found to have a considerably polar character. It can then be trivially shown that the two soft modes have a very similar contribution to the total spontaneous polarization of the $Cmc2_1$ phase of LTO, in spite of the fact that ξ_1 embodies 81% of the PE-to-FE distortion. Hence, the two-mode character of the transition is critical to explain the relatively large \mathbf{P}^S of the $Cmc2_1$ phase.

Unfortunately, we were unable to find experimental results for the ferroelectric and response properties of the $Cmc2_1$ phase of LTO. Table III shows some results for the $P2_1$ phase of the compound that is stable at room temperature. Interestingly, the dielectric and piezoelectric responses measured for this phase seem compatible (at least in magnitude) with our values for $Cmc2_1$. As regards the spontaneous polarization, the value for the $P2_1$ phase is smaller than ours by a factor of 6; this experimental result was essentially confirmed by the first-principles study of Ref. 16, which employed a DFT theory similar to ours.⁴¹ Hence, we can tentatively conclude that the $Cmc2_1$ -to- $P2_1$ transformation, which is experimentally determined to occur at 1053 K,³² involves a reduction of LTO's spontaneous polarization. While such a reduction in the magnitude of \mathbf{P}^S as the temperature decreases is not typical in FE perovskites, in principle there is no reason to question this possibility.

Finally, let us discuss an intriguing possibility suggested by the very different magnitudes of the computed mode charges $\bar{Z}_{1,z}$ and $\bar{Z}_{2,z}$. Since $\bar{\mathbf{Z}}_s$ quantifies the coupling between a polar mode and an applied electric field, we can expect ξ_2 to be much more reactive to an external

bias than ξ_1 . One can thus imagine the following possibility: to apply an electric field to LTO in its $Cmc2_1$ phase and switch *only the part of the spontaneous polarization associated to* ξ_2 . More precisely, if (u_1^I, u_2^I) represents the FE phase discussed so far, an electric field might allow us to take the material into a qualitatively different polarization state $(u_1^{II}, u_2^{II}) \approx (u_1^I, -u_2^I)$. LTO would thus be a four-state ferroelectric, as the $(-u_1^I, -u_2^I)$ and $(-u_1^{II}, -u_2^{II})$ variants would be accessible as well. A necessary condition for such a partial switching to occur is that the (u_1^{II}, u_2^{II}) state be a minimum of the energy. More precisely, we need the coupling between ξ_1 and ξ_2 to be dominated by the $\gamma'' u_1^2 u_2^2$ term of Eq. (2): Note that, for $|\gamma''|$ much greater than $|\gamma'|$ and $|\gamma'''|$, the four states $(\pm u_1^I, \pm u_2^I)$ would have essentially the same energy; in contrast, if γ' or γ''' dominate, the “ ξ_2 -switched” state would have a much higher energy and might not be a minimum of $E(u_1, u_2)$. In order to confirm or disprove such a partial switching, we considered the equilibrium structure of the $Cmc2_1$ phase (i.e., the one reported in Table I) and generated configurations in which the ξ_2 distortion was inverted and given various magnitudes; we relaxed such transformed structures and invariantly obtained the original $Cmc2_1$ phase as final result. Hence, while we did not explore the $E(u_1, u_2)$ energy landscape in detail, our results clearly indicate there is no stable “ ξ_2 -switched” state. Equivalently, this implies that the γ' and γ''' terms of Eq. (2) dominate over γ'' (which supports the assumption made in Section III.C).

E. BaTiO₃-like ferroelectric modes in La₂Ti₂O₇

Thus far we have discussed the main features of LTO’s high-temperature FE transition, showing that this compound is very different from the FE oxides with the ideal perovskite structure. In particular, our results seem to suggest that LTO and BTO have little in common, in spite of the fact that they share the same building block: TiO₆ octahedra with Ti⁴⁺ in the 3d⁰ electronic configuration. In the following we show that such a conclusion would be a deceptive one.

Ferroelectricity in the usual FE perovskite oxides relies on strong dipole-dipole interactions whose fingerprint is the anomalously large magnitude of the Born effective charges of some atomic species.⁴² A prototypical example of this behavior is BTO, for which we computed the effective-charge tensors shown in Table V. Most notably, in the PE phase the Ti⁴⁺ cations display Z^* values above 7e, almost doubling their nominal ionization charge. Analogously, the displacement of the O atoms towards the Ti has a dynamical charge of $-5.77e$ associated to it, almost tripling the nominal value of $-2e$. It is well-known that this effect is related with a partial covalent character of the Ti–O bond, and an increased hybridization of the O-2p and Ti-3d orbitals as the Ti and O atoms approach.¹⁷ Thus, given this chemical origin, the effective charges become less anomalous once the

FE distortion freezes in: according to the results in Table V, Ti’s charge of 7.31e gets reduced to 5.83e, while O’s charge of $-5.77e$ falls to $-4.79e$.

As apparent from Table IV, some Ti and O atoms in LTO also present anomalously large effective charges that reach values similar to those obtained for BTO. In the case of the Ti atoms, the computed Z^* tensors are rather isotropic, with the maximum Z^* values [i.e., 6.91e for Ti(1) and 7.45e for Ti(2)] corresponding to displacements along the in-layer directions x and z . In the case of the O atoms, O(6) and O(7) clearly present the largest values, which exceed $-5e$ as in BTO. Such giant dynamical charges corresponds to displacements along the x direction, for which LTO presents infinite chains of TiO₆ octahedra (see Figs. 1 and 2) as those in the ideal perovskite structure. Hence, as regards their *polarizability* properties, the results for the Ti and O atoms in LTO are strongly reminiscent of the behavior that is well-known for BTO.

Do such anomalous effective charges lead to FE instabilities in LTO? In accordance with the above discussion, the answer to this question is a negative one: the $Cmcm$ phase presents only two Γ -point instabilities (i.e., the already discussed ξ_1 and ξ_2) and the $Cmc2_1$ is stable against Γ -point perturbations.⁴³ Nevertheless, by inspecting the \mathbf{K} -eigenmodes of the $Cmcm$ phase, it is easy to find several low-energy FE modes that are BTO-like, i.e., they involve the displacement of the Ti atoms away from the center of nearly undistorted O₆ octahedra.^{44,45} For example, we found a marginally stable and strongly polar mode for which we computed $\kappa_s = 0.26$ eV/Å² and $Z_{s,x} = 21.7e$ (this distortion is x -polarized and has B_{3u} symmetry); this mode gives an enormous contribution to the ϵ_{xx} dielectric response:⁴⁶ the obtained value exceeds 600. Interestingly, these BTO-like modes become stiffer in the $Cmc2_1$ phase; thus, they do not give raise to any anomalously large contribution to the dielectric response reported in Table III.

In conclusion, our analysis shows that LTO presents obvious traces of the FE instabilities of BTO. Such a *transferability* of instabilities was demonstrated by one of us in an hexagonal polymorph of BTO.⁴⁵ In that case, the FE phase transition was shown to be driven by soft modes that are an almost perfect match of the usual BTO-like FE instability. In LTO, such modes are very low in energy, but still stable; further, they clearly compete with the dominating AFD-like instability, and become stiffer once the $Cmcm$ -to- $Cmc2_1$ transition occurs. Nevertheless, noting that BTO-like FE distortions tend to be very sensitive to cell strains, our results suggest the possibility that such instabilities might be induced in LTO by suitable strain engineering or chemical substitution, or that they might occur spontaneously in similar layered perovskites.

F. Implications for work on magnetoelectrics

Finding materials that display large magnetoelectric (ME) effects (i.e., a large magnetic reaction to an applied electric field) at room temperature is a major challenge that remains to be successfully tackled. The difficulties involved in the design of good magnetoelectrics have been discussed elsewhere.⁴⁷ At present, the strategies that seem most promising rely on finding systems that satisfy the following two conditions: (1) their atomic structure must react strongly to an applied electric field (i.e., we are looking for good dielectrics), and (2) the field-induced distortions must have a large effect on the magnetic interactions (as emphasized in Refs. 48 and 49).

While there are well-known strategies to comply with the first condition,⁴⁷ satisfying the second one is proving much more difficult. In fact, the existing quantitative studies indicate that the dielectric response of ME multiferroics like BiFeO₃ is dominated by modes that have small magnetostructural couplings associated to them.⁵⁰ It is thus interesting to consider the alternative approach adopted by Benedek and Fennie.¹³ These authors noted that modes involving O₆ rotations are likely to be strongly coupled with the magnetism of perovskite oxides, as such AFD-like distortions usually control the nature and magnitude of the main magnetic interactions (e.g., the metal–oxygen–metal super-exchange and Dzyaloshinskii-Moriya couplings). Hence, they looked for materials in which AFD-like distortions are related with (or lead to) ferroelectricity, as in such cases one could use an electric field to act upon the O₆ rotations. Note that the sought connection between AFD-like distortions and ferroelectricity is an exotic one, since the O₆-rotational modes are strictly non-polar in compounds with the ideal perovskite structure (see Section III.B). Accordingly, ferroelectricity-related O₆-rotational modes have been found in non-ideal perovskites, e.g., in the PbTiO₃/SrTiO₃ artificial superlattices⁶ and the layered compound Ca₃Mn₂O₇.¹³ In both cases, ferroelectricity has an *improper* character, and a combination of various AFD-like modes must occur for an spontaneous polarization to appear.

There is no need to emphasize the importance of our findings for LTO in the context of magnetoelectrics. In LTO's case, the FE soft mode is AFD-like already; hence, it can freeze in and give raise to a sizeable spontaneous polarization by itself, without the need of any accompanying distortion. Further, LTO's O₆ rotations couple directly (bi-linearly) with an applied electric field, which might prove advantageous for the purpose of obtaining large ME effects. (In improper ferroelectrics, the coupling between an applied field and the AFD-like modes will typically be a higher-order effect.) Indeed, the *proper ferroelectricity driven by O₆ rotations* that occurs in LTO seems to be the dreamed FE instability from the viewpoint of ME applications.

One would thus like to obtain LTO-like ferroelectricity in a magnetic material. The most obvious possibil-

ity is to consider the substitution of Ti by Mn in LTO, so as to form La₂Mn₂O₇, a crystal that we have not found described in the literature. In La₂Mn₂O₇ we would have manganese in the Mn⁴⁺ ionization state, most likely in the high spin $t_{2g}^3e_g^0$ electronic configuration; thus, we can expect this crystal to be insulating. Further, since the Ti–O chemistry does not seem to play any relevant role in LTO's FE instability, we can expect La₂Mn₂O₇ to present a FE transition analogous to LTO's. Hence, this material seems an excellent candidate to satisfy the condition (2) mentioned above and thus display large ME effects. Additionally, one would like the FE transition to occur near room temperature, so as to benefit from the enhancement of the functional responses near T_C [in the spirit of the condition (1) mentioned above]. In this sense, it may be useful to note that materials like Sr₂Ta₂O₇⁵¹ or Sr₂Nb₂O₇⁵² present FE transitions that seem similar to LTO's but occur at lower T_C 's: 166 K and 1615 K, respectively. This suggests that exploring alternative compositions is a promising route to tune the temperature of the O₆-rotational FE transition.

IV. SUMMARY AND CONCLUSIONS

We used first-principles methods to study the origin of ferroelectricity in the layered perovskite La₂Ti₂O₇ (LTO), one of the materials with highest Curie temperature known ($T_C = 1770$ K). To do so, we carried out for LTO a research program that has been repeatedly and successfully applied to the investigation of displacive phase transitions in ferroelectric (FE) oxides with the perovskite structure. Our results allowed us to characterize LTO's high-temperature FE transition, which was found to present very peculiar features.

We found that ferroelectricity in LTO is very different from what occurs in the well-known FE oxides with the ideal perovskite structure, such as BaTiO₃ (BTO) or PbZr_{1-x}Ti_xO₃ (PZT). Indeed, the dominant FE instability of this compound has little in common with the textbook picture of positive charges moving against negative charges in an ionic insulator; instead, it involves concerted rotations of the oxygen octahedra that form the perovskite framework. Hence, LTO's high-temperature structural transition is reminiscent of the behavior of simple perovskite oxides, but not the FE ones: LTO's FE distortion is much alike the O₆ rotational soft modes that drive the *anti-ferrodistortive* phase transitions of SrTiO₃, LaAlO₃, LaMnO₃, and many other *non-polar* perovskite crystals.

Hence, we found that the existence of ferroelectricity in LTO at record-high temperatures is the result of structural distortions as those occurring in many perovskite oxides that are *not* ferroelectric. As discussed here, the solution to this puzzle has to do with LTO's layered structure: Because the lattice of oxygen octahedra is truncated in this compound, the O₆-rotations acquire a polar character and give raise to a macroscopic polarization.

We can thus describe LTO as a *topological ferroelectric*, since it owes its spontaneous polarization to the layered topology of its structure. Note that such a peculiar topology does not seem essential for LTO's high-temperature transition to occur, but it is critical for it to have a ferroelectric character.

We quantified energetics of LTO's FE transformation, the results being consistent with the very high temperature at which it happens. Most remarkably, we found that the structural distortion connecting the PE ($Cmcm$) and FE ($Cmc2_1$) phases presents large contributions from two modes, namely, the above-mentioned strong instability consisting of O_6 rotations, and an isosymmetric weakly-unstable mode that involves deformations of the oxygen octahedra. Further, we found that the large energy change associated to the $Cmcm$ -to- $Cmc2_1$ transition depends crucially on the simultaneous occurrence of both modes. We were able to describe such effects in terms of a very strong and *cooperative* anharmonic coupling, and briefly discussed the possibility of constructing a phenomenological theory of such a *two-mode transition*. Interestingly, LTO's behavior is in strong contrast with what (to the best of our knowledge) is most common among perovskite oxides, where structural instabilities tend to compete and suppress each other.

We calculated the polarization and response properties of LTO's FE phase, obtaining results that are consistent with related experimental information. Interestingly, the computed electric properties revealed clear similarities between LTO and prototype ferroelectric BTO. For example, we obtained anomalously large Born effective charges for some Ti and O atoms in LTO, a feature that is known to be the fingerprint of the FE instabilities in compounds like BTO and PZT. Further, our results showed that LTO presents nearly-unstable modes that are strongly polar and involve atomic distor-

tions that essentially match BTO's FE instabilities. Such traces of BTO-like behavior in LTO suggest the intriguing possibility that *conventional* ferroelectricity might be induced in this compound upon suitable modifications (e.g., strain engineering or chemical substitutions), or that such a behavior might occur spontaneously in similar materials.

Finally, let us emphasize the implications that our findings have for the design of new magnetoelectric multiferroics. In the context of magnetoelectric perovskite oxides, it would be ideal to have proper ferroelectricity driven by O_6 -rotational modes, so that an electric field can be used to tune the structural distortions (e.g., metal-oxygen-metal angles) that control the main magnetic interactions (i.e., super-exchange and Dzyaloshinskii-Moriya). That is exactly the kind of ferroelectricity that we have found in LTO. Here we have briefly discussed how to obtain such an effect in a magnetic perovskite, proposing $La_2Mn_2O_7$ as the most promising candidate material.

In conclusion, our theoretical study of $La_2Ti_2O_7$ has revealed a wealth of interesting effects, some of which may have important implications for current work on multifunctional oxides. We thus hope this study will stimulate further investigation of these layered perovskites and the novel functionalities that they may offer.

This work was supported by MICINN-Spain (Grants No. MAT2010-18113, No. MAT2010-10093-E, and No. CSD2007-00041) and CSIC's JAE-pre program (J.L.P.). We used the supercomputing facilities provided by CESGA, the tools provided by the Bilbao Crystallographic Server,⁵³ and the VESTA software⁵⁴ for the preparation of some figures. We gratefully acknowledge discussions with E. Canadell, M. Stengel, and J.C. Wojdeł.

-
- ¹ M.E. Lines and A.M. Glass, *Principles and applications of ferroelectrics and related materials* (Oxford Univ. Press 1977, 2001).
- ² G.A. Samara, *Sol. St. Phys.* **56**, 240 (2001).
- ³ K.M. Rabe, C.H. Ahn, and J.-M. Triscone (Eds.), *Physics of ferroelectrics, a modern perspective* (Springer-Verlag, Berlin Heidelberg 2007).
- ⁴ K.M. Rabe and P. Ghosez, *Topics Appl. Phys.* **105**, 117 (2007).
- ⁵ J. Junquera and P. Ghosez, *J. Comp. Theo. Nanosci.* **5**, 2071 (2008).
- ⁶ E. Bousquet *et al.*, *Nature* **452**, 732 (2008).
- ⁷ M. Fiebig, *J. Phys. D: Appl. Phys.* **38**, R123 (2005).
- ⁸ A. Filippetti and N.A. Hill, *Phys. Rev. B* **65**, 195120 (2002).
- ⁹ S. Bhattacharjee, E. Bousquet, and Ph. Ghosez, *Phys. Rev. Lett.* **102**, 117602 (2009).
- ¹⁰ G. Catalan and J.F. Scott, *Adv. Mats.* **21**, 2463 (2009).
- ¹¹ B.B. Van Aken, T.T.M. Palstra, A. Filippetti, and N.A. Spaldin, *Nat. Mat.* **3**, 164 (2004).
- ¹² C.J. Fennie and K.M. Rabe, *Phys. Rev. B* **72**, 100103 (2005).
- ¹³ N.A. Benedek and C.J. Fennie, arxiv.org/abs/1007.1003.
- ¹⁴ S. Nanamatsu, M. Kimura, K. Doi, S. Matsushita, and N. Yamada, *Ferroelectrics* **8**, 511 (1974).
- ¹⁵ H. Yan, H. Ning, Y. Kan, P. Wang, and M.J. Reece, *J. Am. Cer. Soc.* **92**, 2270 (2009).
- ¹⁶ E. Bruyer and A. Sayede, *J. Appl. Phys.* **108**, 053705 (2010).
- ¹⁷ M. Posternak, R. Resta, and A. Baldereschi, *Phys. Rev. B* **50**, 8911 (1994).
- ¹⁸ P. Ghosez, E. Cockayne, U.V. Waghmare, and K.M. Rabe, *Phys. Rev. B* **60**, 836 (1999).
- ¹⁹ F. Lichtenberg, A. Hernberger, K. Wiedenmann, and J. Mannhart, *Prog. Sol. St. Chem.* **29**, 1 (2001).
- ²⁰ C.N.R. Rao and B. Raveau, *Transition metal oxides (2nd Ed.)* (John Wiley & Sons Inc. 1998).
- ²¹ R.D. King-Smith and D. Vanderbilt, *Phys. Rev. B* **49**, 5828 (1994).
- ²² In several publications it is assumed that the high-

- temperature phase of LTO presents the $Cmcm$ space group, and the literature is cited for supposed experimental proof of this fact. However, we have carefully checked the literature and were unable to find any results concerning the crystal structure of LTO's PE phase.
- ²³ S.C. Abrahams and E.T. Keve, *Ferroelectrics* **2**, 129 (1971).
- ²⁴ E. Kroumova, M.I. Aroyo, and J.M. Pérez-Mato, *Acta Cryst. B* **58**, 921 (2002).
- ²⁵ E. Kroumova *et al.*, *J. Appl. Cryst.* **34**, 783 (2001); we also used the tools available in the "Materials Studio" software package (Accelrys, Inc.).
- ²⁶ S.C. Abrahams, S.K. Kurtz, and P.B. Jamieson, *Phys. Rev. B* **172**, 551 (1968).
- ²⁷ S. Nanamatsu, M. Kimura, K. Doi and M. Takahashi, *J. Phys. Soc. Jap.* **30**, 300 (1971).
- ²⁸ J.K. Brandon and H.D. Megaw, *Phil. Mag.* **21**, 189 (1970).
- ²⁹ G. Kresse and J. Furthmuller, *Phys. Rev. B* **54**, 11169 (1996); G. Kresse and D. Joubert, *Phys. Rev. B* **59**, 1758 (1999).
- ³⁰ P.E. Blochl, *Phys. Rev. B* **50**, 17953 (1994); G. Kresse and D. Joubert, *Phys. Rev. B* **59**, 1758 (1999).
- ³¹ X. Wu, D. Vanderbilt, and D.R. Hamann, *Phys. Rev. B* **72**, 035105 (2005).
- ³² N. Ishizawa, F. Marumo, S. Iwai, M. Kimura, and T. Kawamura, *Acta Cryst. B* **38**, 368 (1982).
- ³³ A.M. Glazer, *Acta Cryst. B* **28**, 3384 (1972).
- ³⁴ C. Howard and H.T. Stokes, *Acta Cryst. A* **61**, 93 (2004).
- ³⁵ See e.g. O. Diéguez, O.E. González-Vázquez, J.C. Wojdeł, and J. Íñiguez (arxiv.org/abs/1011.0563) and references therein.
- ³⁶ In the usual perovskite oxides, the coupling between the FE modes and strain tends to be stronger than the AFD-strain coupling. For example, Fig. 1 of Ref. 9 illustrates these effects as computed for CaMnO_3 ; the FE-strain coupling is very significant, while the AFD-strain interaction is almost negligible. These couplings have been quantified in detail for SrTiO_3 : King-Smith and Vanderbilt²¹ computed FE-strain couplings of about 0.0036 hartree/bohr⁵, while Sai and Vanderbilt [*Phys. Rev. B* **62**, 13942 (2000)] obtained AFD-strain couplings of about 0.0002 hartree/bohr⁵.
- ³⁷ The fourth-order expression in Eq. (2) may not be good description of the energy for arbitrary values of u_1 and u_2 ; e.g., distortions with $u_1 = u_2$ are unbounded from below for the fitted parameter values. An acceptable description of the full $E(u_1, u_2)$ energy landscape would probably require including higher order terms.
- ³⁸ W. Zhong and D. Vanderbilt, *Phys. Rev. Lett.* **74**, 2587 (1995).
- ³⁹ The $Q_1^3 Q_2$ term guarantees that both Q_1 and Q_2 will freeze in at T_C .
- ⁴⁰ R.D. King-Smith and D. Vanderbilt, *Phys. Rev. B* **47**, 1651 (1993).
- ⁴¹ The authors of Ref. 16 used a generalized-gradient approximation (GGA) to DFT. As compared with the LDA employed in this work, GGA is known to overestimate the structural distortion and spontaneous polarization in the usual FE perovskites – see e.g. Bilec *et al.* [*Phys. Rev. B* **77**, 165107 (2008)] and references therein. Hence, while LTO is not an usual ferroelectric, it seems fair to conclude that, according to the results of Ref. 16 and ours, the spontaneous polarization of the $Cmc2_1$ phase is significantly larger than that of the $P2_1$ phase.
- ⁴² W. Zhong, R.D. King-Smith, and D. Vanderbilt, *Phys. Rev. Lett.* **72**, 3618 (1994).
- ⁴³ The $Cmc2_1$ phase might present structural instabilities associated to the $Cmc2_1$ -to- $P2_1$ transition that is known to occur in LTO. Such a transition involves the doubling of the $Cmc2_1$ cell along the x direction. Thus, the $Cmc2_1$ -to- $P2_1$ transformation is driven by a non- Γ distortion; such distortions were not considered in the present study.
- ⁴⁴ To quantify the resemblance between the TiO_6 distortions in BTO and LTO, we projected the corresponding atomic displacements of the \mathbf{K} -eigenmodes of LTO's $Cmcm$ phase into the distortion pattern derived from the FE soft mode of BTO's $Pm\bar{3}m$ phase. This kind of analysis is described in more detail in Ref. 45.
- ⁴⁵ J. Íñiguez, A. García, and J.M. Pérez-Mato, *J. Phys.: Condens. Matt.* **12**, L387 (2000).
- ⁴⁶ The lattice dielectric response can be split in mode contributions as $\epsilon_{\alpha\beta} = \Omega^{-1} \sum_s \bar{Z}_{s,\alpha} \bar{Z}_{s,\beta} \kappa_s^{-1}$, in units of ϵ_0 and where Ω is the cell volume.
- ⁴⁷ J.C. Wojdeł and J. Íñiguez, *Phys. Rev. Lett.* **105**, 037208 (2010).
- ⁴⁸ C.J. Fennie, *Phys. Rev. Lett.* **100**, 167203 (2008).
- ⁴⁹ K.T. Delaney, M. Mostovoy, and N.A. Spaldin, *Phys. Rev. Lett.* **102**, 157203 (2009).
- ⁵⁰ J.C. Wojdeł and J. Íñiguez, *Phys. Rev. Lett.* **103**, 267205 (2009).
- ⁵¹ N. Ishizawa, F. Marumo, T. Kawamura, and M. Kimura, *Acta Cryst. B* **32**, 2564 (1976).
- ⁵² N. Ishizawa, F. Marumo, T. Kawamura, and M. Kimura, *Acta Cryst. B* **31**, 1912 (1975).
- ⁵³ M. I. Aroyo *et al.*, *Z. Krist.* **221**, 15 (2006); M. I. Aroyo, A. Kirov, C. Capillas, J.M. Perez-Mato, and H. Wondratschek, *Acta Cryst. A* **62**, 115 (2006).
- ⁵⁴ K. Momma and F. Izumi, *J. Appl. Cryst.* **41**, 653 (2008).